Journal of Visualized Experiments

Characterization and Functional Prediction of Bacteria in Ovarian Tissues

--Manuscript Draft--

Article Type:	Invited Methods Article - Author Produced Video
Manuscript Number:	JoVE61878R4
Full Title:	Characterization and Functional Prediction of Bacteria in Ovarian Tissues
Corresponding Author:	Qiling Li, Ph.D. Xi'an Jiaotong University Xi'an, CHINA
Corresponding Author's Institution:	Xi'an Jiaotong University
Corresponding Author E-Mail:	liqiling@mail.xjtu.edu.cn
Order of Authors:	Lanbo Zhao
	Weichu Zhao
	Qi Wang
	Dongxin Liang
	Yu Liu
	Guoxing Fu
	Lu Han
	Yiran Wang
	Chao Sun
	Qing Wang
	Qing Song
	Qiling Li, Ph.D.
	Qinrui Lu
Additional Information:	
Question	**Response**
Please indicate whether this article will be Standard Access or Open Access.	Standard Access (US$1200)
Please confirm that you have read and agree to the terms and conditions of the author license agreement that applies below:	I agree to the Author License Agreement
Please specify the section of the submitted manuscript.	Cancer Research
Please indicate whether this article will be Standard Access or Open Access.	Standard Access ($1400)
Please confirm that you have read and agree to the terms and conditions of the video release that applies below:	I agree to the Video Release
Please provide any comments to the journal here.	

TITLE:

Characterization and Functional Prediction of Bacteria in Ovarian Tissues

AUTHORS AND AFFILIATIONS:

Lanbo Zhao[1]*, Weichu Zhao[2]*, Qi Wang[1]*, Dongxin Liang[1], Yu Liu[3],Guoxing Fu[4], Lu Han[1], Yiran Wang[1], Chao Sun[1], Qing Wang[1], Qing Song[1], Qiling Li[1], Qinrui Lu[1]

*These authors contributed to this work equally.

[1]Department of Obstetrics and Gynecology, First Affiliated Hospital of Xi'an Jiaotong University, Xi'an, Shannxi, China

[2]School of Social Sciences, University of Manchester, Manchester, UK

[3]Department of Pathology, First Affiliated Hospital of Xi'an Jiaotong University, Xi'an, Shannxi, China

[4]Omega Bioservices Inc, Norcross, GA, USA

Email addresses of co-authors:

Lanbo Zhao (boboup2u@stu.xjtu.edu.cn)

Weichu Zhao (weichu.zhao@student.manchester.ac.uk)

Qi Wang (wangqiw@stu.xjtu.edu.cn)

Corresponding author:

Qiling Li (liqiling@mail.xjtu.edu.cn)

Qinrui Lu(junhuacao610@163.com)

KEYWORDS:

Ovarian cancer, Bacteria, 16S rRNA gene sequencing, Lipopolysaccharide, KEGG, Immunohistochemistry

SUMMARY:

Immunohistochemistry staining and 16S ribosomal RNA gene (16S rRNA gene) sequencing were performed in order to discover and distinguish bacteria in cancerous and noncancerous ovarian tissues in situ. The compositional and functional differences of the bacteria were predicted by using BugBase and Phylogenetic Investigation of Communities by Reconstruction of Unobserved States (PICRUSt).

ABSTRACT:

The theory of a "sterile" female upper reproductive tract has been encountering increasing opposition due to advancements in bacterial detection. However, whether ovaries contain bacteria has not yet been confirmed yet. Herein, an experiment to detect bacteria in ovarian tissues was introduced. We chose ovarian cancer patients in the cancer group and noncancerous patients in the control group. 16S rRNA gene sequencing was used to differentiate bacteria in ovarian tissues from the cancer and control groups. Furthermore, we predicted the functional composition of the identified bacteria by using BugBase and PICRUSt. This method can also be used in other viscera and tissues since many organs have been

proven to harbor bacteria in recent years. The presence of bacteria in viscera and tissues may help scientists evaluate cancerous and normal tissues and may be aid in the treatment of cancer.

INTRODUCTION:

Recently, an increasing number of articles have been published that prove the existence of bacteria in abdominal solid viscera, such as the kidney, spleen, liver, and ovary[1,2]. Geller *et al.* found bacteria in pancreatic tumors, and these bacteria were resistant to gemcitabine, a chemotherapeutic drug[2]. S. Manfredo Vieira *et al.* concluded that *Enterococcus gallinarum* was portable to the lymph nodes, liver and spleen, and it could drive autoimmunity[3].

Since the cervix plays a role as a defender, bacteria in the upper female reproductive tract, which contains the uterus, fallopian tubes, and ovaries, have been minimally researched. However, some new theories have been established in recent years. Bacteria may have access to the uterine cavity during the menstrual cycle due to changes in mucins[4,5]. Additionally, Zervomanolakis *et al.* confirmed that the uterus, together with the fallopian tubes, is a peristaltic pump controlled by the endocrine system of the ovaries, and this arrangement enables bacteria to enter the endometrium, fallopian tubes, and ovaries[6].

The upper reproductive tract is no longer a mystery anymore thanks to the development of bacterial detection methods. Verstraelen *et al.* used a barcoded paired-end sequencing method to discover uterine bacteria by targeting at the V1-2 hypervariable region of the 16S RNA gene[7]. Fang *et al.* employed barcoded sequencing in patients with endometrial polyps and revealed the presence of diverse intrauterine bacteria[8]. Additionally, by using the 16S RNA gene, Miles *et al.* and Chen *et al.* found bacteria in the genital system of women who had undergone salpingo-oophorectomy and hysterectomy, respectively[5,9].

Bacteria in tumor tissues have gained increasing attention in recent years. Banerjee *et al.* discovered that the microbiome signature differed between ovarian cancer patients and controls[10]. A*noxynatronum sibiricum* was associated with tumor stage, and *Methanosarcina vacuolata*might may be used to diagnose ovarian cancer[11]. In addition to ovarian cancer, other cancers, such as stomach, lung, prostate, breast, cervix, and endometrium, have been proven to be associated with bacteria[12-18]. Poore *et al.* proposed a new class of microbial-based oncology diagnostics, foreseeing early-stage cancer screening[19]. In this protocol, we investigated the differences between cancerous and normal ovarian tissues by comparing the composition and function of bacteria in these two tissues.

Immunohistochemistry staining and 16S rRNA gene sequencing were performed to confirm the presence of bacteria in the ovaries. The differences and predicted functions of the ovarian bacteria in cancerous and noncancerous ovarian tissues were studied. The results showed the existence of bacteria in ovarian tissues. *Anoxynatronum sibiricum* and *Methanosarcina vacuolata* were related to the stage and the diagnosis of ovarian cancer, respectively. Forty-six significantly different KEGG pathways that were present in both groups were compared.

PROTOCOL:

This study was approved by the Medical Institutional Ethics Committee of the First Affiliated Hospital of Xi'an Jiaotong University (No. XJTUIAF2018LSK-139). Informed consent was obtained from all enrolled patients.

1 Criteria for entering the cancer group and the control group

1.1.1 For the cancer group, enroll patients who are primarily diagnosed with ovarian cancer, and after laparotomy, they are proven to have serous ovarian cancer by pathological findings.

1.1.2 For the control group, enroll patients that are primarily diagnosed with uterine myoma or uterine adenomyosis, without presenting any ovarian condition, and who have undergone hysterectomy and salpingo-oophorectomy.

NOTE: This standard is not definite. Patients with diseases not affecting the ovaries who undergo hysterectomy and salpingo-oophorectomy can also be enrolled.

1.2 Exclude patients with one or more of the following criteria:
Pregnant or breast-feeding women.
Taking antibiotics 2 months prior to the surgery.
Having fever or elevated inflammatory markers.
Having inflammation of any kind.
Having undergone neoadjuvant chemotherapy.

2 Gather samples

2.1 During the surgery, place the resected ovaries into a sterile tube and place the tube in liquid nitrogen for transport. Avoid touching anything else throughout the whole procedure.

2.2 Separate the ovaries into approximately 1-cm thick tissue samples with a pair of new sterile tweezers under a laminar flow cabinet. After separation, preserve samples at -80 °C.

NOTE: All the procedures for gathering samples are aseptic, including separating the ovaries.

3 Sequence the 16S rRNA gene

3.1 Extract DNA.

3.1.1 Add 1.2 mL of inhibit EX buffer into a 2 mL centrifuge tube. Then, add 180-220 mg of samples into the tube. Let the sample fully mix (70 °C water bath for 5 min and then vortex for 15 s).

3.1.2 Centrifuge the tube for 1 min at 600 x g.

3.1.3 Place 550 µL of the supernatant into a new 1.5 mL tube, and centrifuge for 1 min at 600 x g.

3.1.4 Transfer 400 µL of the supernatant with 30 µL of proteinase K into another 1.5 mL tube.

3.1.5 Add 400 µL of buffer AL and use a vortex mixer for 15 s.

3.1.6 Incubate at 70 °C for 10 min.

3.1.7 Add 400 µL of 96-100% alcohol. Use a vortex mixer for 15 s.

3.1.8 Transfer 600 µL of mixture into an absorption column and centrifuge for 1 min at 13700 g. Exchange the lower tube. Repeat this step 11 times.

3.1.9 Add 500 µL of buffer AW1, centrifuge for 1 min at 13,700 x g, and change the lower tube.

3.1.10 Add 500 µL of buffer AW2, centrifuge for 3 min at 13,700 x g, and change the lower tube.

3.1.11 Centrifuge for 3 min at 13,700 x g.

3.1.12 Transfer the mixture into a new 1.5 mL tube, add 200 µL of buffer ATE, incubate at room temperature for 5 min and centrifuge for 1 min at 13,700 x g.

3.2 Quality testing. Use 1% Sepharose gel electrophoresis to test the quality. Add 400 ng of sample, 120 V, 30 mins. Ideal result: DNA concentration: ≥ 10 ng/µL, DNA purity: A260/A280 = 1.8-2.0, gross DNA: ≥ 300 ng.

3.3 Prepare the libraries using a 16S metagenomic sequencing kit according to the manufacturer's protocol.

3.3.1 Perform PCR. Briefly, each 25 µL PCR reaction contains 12.5 ng of sample DNA as input, 12.5 µL of 2x KAPA HiFi HotStart ReadyMix and 5 µL of each primer at 1 µM.

3.3.2 Carry out PCR using the following protocol: an initial denaturation step performed at 95°C for 3 min followed by 25 cycles of denaturation (95°C, 30 s), annealing (55°C, 30 s) and extension (72°C, 30 s), and a final elongation of 5 min at 72°C.

3.3.3 Clean up the PCR product from the reaction mix with magnetic beads using the manufacturer's instructions.

3.3.4 Repeat steps 3.3.1 and 3.3.2.

3.3.5 Quality testing. Please refer to step 3.2.

3.3.6 Repeat step 3.3.3.

3.3.7 Quality testing. Use 1% Sepharose gel electrophoresis to test impurity, a spectrophotometer to test purity, a fluorometer to test the concentration, and an RNA assay kit to test integrity. Follow the manufacturer's protocol. Normalize and pool the libraries; then sequence (2 x 300 bp paired-end read setting) using 600 cycle V3 standard flow cells, producing approximately 100,000 paired-end 2 x 300 base reads.

NOTE: The full-length primer sequences: 16S Amplicon polymerase chain reaction (PCR) Forward primer: 5' TCGTCGGCAGCGTCAGATGTGTATAAGA GACAG-[CCTACGGGNGGCWGCAG] and 16S Amplicon PCR Reverse primer: 5' GTCTCGTGGGCTCGGAGATGTGTATAAGAGACAG-[GACTACHVGGGTATCTAATCC].

4 Analyze 16S rRNA gene sequencing data

4.1 Filter the raw reads of every sample based on sequencing quality with the software package QIIME 2-201802[20].

4.1.1 Copy three files into the directory: emp-paired-end-sequences_01
one **forward.fastq.gz** file that contains the forward sequence reads,
one **reverse.fastq.gz** file that contains the reverse sequence reads,
one **barcodes.fastq.gz** file that contains the associated barcode reads

4.1.2 Execute

```
qiime tools import \
--type EMPPairedEndSequences \
--input-path emp-paired-end-sequences_01 \--output-path emp-paired-end-sequences_02.qza
```

4.2 Remove the primer and adaptor sequences.

```
qiime cutadapt trim-paired \
--i-demultiplexed-sequences demultiplexed-seqs_02.qza \
--p-front-f GCTACGGGGGG \
--p-front-r GCTACGGGGGG \
--p-error-rate 0 \
--quality-cutoff 25 \
--o-trimmed-sequences trimmed-seqs_03.qza \
--verbose
```

4.3 Shorten sequence reads in which both paired-end qualities are lower than 25. See above --quality-cutoff 25

4.4 Analyze the sequencing data.

4.4.1 Gather sequences to form operational taxonomic units (OTUs) with a similarity cutoff at 97%.

```
qiime vsearch dereplicate-sequences \
--i-sequences trimmed-seqs_03.qza \
--o-dereplicated-table table_04.qza \
--o-dereplicated-sequences rep-seqs_04.qza

qiime vsearch cluster-features-closed-reference \
--i-table table_04.qza \
--i-sequences rep-seqs_04.qza \
--i-reference-sequences 97_otus.qza \
--p-perc-identity 0.97 \
--o-clustered-table table-cr-97.qza \
--o-clustered-sequences rep-seqs-cr-97.qza \
--o-unmatched-sequences unmatched-cr-97.qza
```

4.4.2 For the OTUs, calculate the relative abundance in each sample. Abundance information is in table-cr-97.qza

4.5 Employ a native Bayesian classifier, which aims at the RDP training set (version 9; http://sourceforge.net/projects/rdp-classifier/), to sort all of the sequences. Mapped taxon information is in table-cr-97.qza

4.6 Within the given OTU, assign a classification that reflects the major coherence of the sequences to OTUs. Then, align the OTUs. See table-cr-97.qza and rep-seqs-cr-97.qza

4.7 Based on the sample group information, perform alpha diversity (including the Chao 1, ACE, Shannon, Simpson and Evenness indexes) and the UniFrac-based principal coordinates analysis (PCoA).

```
qiime tools export \
--input-path table-cr-97.qza \
--output-path exported-feature-table
exported-feature-table

qiime diversity alpha \
--i-table table-cr-97.qza \
--p-metric observed_otus \
--o-alpha-diversity observed_otus_vector.qza

qiime diversity beta \
--i-table table-cr-97.qza \
```

```
--p-metric braycurtis \
--o-distance-matrix unweighted_unifrac_distance_matrix.qza
```

5 Predict bacterial function

5.1 To predict the related representation of the characteristics of the bacteria, use BugBase[21]. The input OTU table for BugBase is prepared using the following commands.

```
biom convert -i otu_table.biom -o otu_table.txt --to-tsv
biom convert -i otu_table.txt -o otu_table_json.biom --table-type="OTU table" --to-json
```

NOTE：The prediction is based on six phenotype categories (Ward*et al.* unpublished) (https://bugbase.cs.umn.edu/): Gram staining, oxygen tolerance, ability to form biofilms, mobile element content, pathogenicity, and oxidative stress tolerance.

5.2 Predict the functional composition of a metagenome by PICRUSt with the usage of marker gene data and a database containing reference genomes[22].

```
make_otu_table.py -i microbiome_97/uclust_ref_picked_otus/test_paired_otus.txt -t /mnt/nas_bioinfo/ref/qiime2_ref/97_otu_taxonomy.txt -o otu_table.biom &
normalize_by_copy_number.py -i otu_table.biom -o normalized_otus.biom
predict_metagenomes.py -i normalized_otus.biom -o metagenome_predictions.biom
categorize_by_function.py -i metagenome_predictions.biom -c "KEGG_Pathways" -l 1 -o picrust_L1.biom
categorize_by_function.py -f -i metagenome_predictions.biom -c KEGG_Pathways -l 1 -o metagenome_predictions.L1.txt
```

5.3 Analyze the differences in functions among each group with the help of STAMP[23,24]. Please refer to the citations to operate the software.

6 Data

6.1 Use statistical software to calculate the significance of the findings. The indication of statistical significance should be set as $P < 0.05$.

6.2. Assess differences in age and parity by Student's t-test. Assess differences in menopausal status, history of hypertension and diabetes by the chi-square test. Assess differences in the number of ovarian bacterial taxa by the Mann-Whitney U test.

REPRESENTATIVE RESULTS:

Patients

A total of 16 qualified patients were included in the study. The control group included 10 women with a diagnosis of benign uterine tumor (among them, 3 patients were diagnosed with uterine myoma, and 7 patients were diagnosed with uterine adenomyosis). Meanwhile, the cancer group contained 6 women with a diagnosis of serous ovarian cancer (among them, 2 patients were diagnosed with stage II, and 2 of them were diagnosed with stage III). The

following characteristics showed no differences between patients in the control group and the cancer group: age, menopausal status, parity, history of hypertension, and history of diabetes (**Table 1**).

[Table 1 here.]

The richness and variety of ovarian bacterial species in both groups

The alpha diversity of the microbes was analyzed as a method to detect the richness and variety of ovarian bacterial species. The number of species observed in the ovarian cancer tissues was smaller than that of the control group, with no significant difference. The richness (represented by the Chao 1 and ACE index) and the diversity (represented by the Shannon, Simpson, and Evenness index) of the bacterial species were both not significantly different between the cancer group and the control group (**Figure 2**).

[Figure 2 here.]

Description of ovarian bacteria

Deep sequencing of the V3-V4 16S rRNA gene region was performed on all samples to obtain a better understanding of the ovarian bacteria. The results showed that *Proteobacteria* was the most abundant phylum (67.10% in the control group and 67.20% in the cancer group), *Firmicutes* was the second most abundant phylum (23.77% in the control group and 23.82% in the cancer group), and the third most abundant phylum was *Bacteroidetes* (3.26% in the control group and 3.41% in the cancer group). When analyzing species of the control group, the main composition was consisted of *Halobacteroides halobios* (14.53%), followed by *Gemmata obscuriglobus* (11.07%) and *Methyloprofundus sedimenti* (10.69%). For the cancer group, *Gemmata obscuriglobus* was the richest in the cluster (13.89%), followed by *Halobacteroides halobius* (11.99%) and *Methyloprofundus sedimenti* (11.12%) (**Figure 3**).

[Figure 3 here.]

Different compositions of ovarian bacteria between the two groups

A comparison of different bacterial communities was carried out by PCoA using PERMANOVA. The results showed that the bacteria in the control group differed from those in the cancer group, $P < 0.05$ (**Figure 4**).

[Figure 4 here.]

Ovarian bacterial composition in cancer and control groups from different perspectives

An analysis of the ovarian bacterial composition was performed from different perspectives to further detect the differences in the identified ovarian bacteria. In **Table 2**, phylum, class, order, family, genus, and species levels were considered, and statistics are provided in the chart. In particular, there was an association between the relative abundance of *Anoxynatronum sibiricum* and the stage of the tumor, and *Methanosarcina vacuolata* was a specific sign when diagnosing ovarian cancer (**Table 2**).

353
354 **Phenotypic conservation of ovarian bacteria in the two groups based on predicted functions**
355 In the cancer group, the expression of genes related to potentially pathogenic and oxidative
356 stress-tolerant phenotypes was increased compared with that of the control group (Wilcoxon
357 signed-rank test, P =0.02 and P =0.002). No significant difference was found between the
358 ovarian cancer and control groups in the following aspects: the phenotypes of aerobic,
359 anaerobic, facultatively anaerobic, gram-positive, and gram-negative bacteria; mobile
360 elements; and biofilm formation of the ovarian bacteria (**Figure 5**). Forty-six variant KEGG
361 pathways between the bacteria in ovaries in the cancer and control groups were determined.
362 The ovaries in the cancer group showed 26 increased pathways. Among them, the most highly
363 related pathways were transporters. On the other hand, the bacteria in ovarian cancer tissue
364 showed 20 reduced pathways. The most relevant functions were as follows: secretion system,
365 unknown functions, and two-component system. The rest of the pathways are shown in
366 **Figure 6**.
367
368 **FIGURE AND TABLE LEGENDS:**
369 **Figure 1: LPS immunohistochemical expression in ovaries.** (A) Control group (10 x). Scale bars,
370 200 µm. (B) Control group (40 x). Scale bars, 50 µm. (C) Cancer group (10x). Scale bars, 200
371 µm. (D) Cancer group (40 x). Scale bars, 50 µm. Arrows point to LPS staining in the ovarian
372 tissue. We obtained reprint permission from previous publishers. This figure has been
373 modified from Wang et al.[11].
374
375 **Figure 2: 16S rRNA gene sequencing shows differences between the cancer and control**
376 **groups in bacterial richness and diversity.** (A) Observed species index (P = 0.06, Mann-
377 Whitney U test); (B) Chao 1 index (P = 0.06, Mann-Whitney U test); (C) ACE index (P = 0.06,
378 Mann-Whitney U test); (D) Shannon index (P = 0.32, Mann-Whitney U test; E. Evenness index
379 (P = 0.48, Mann-Whitney U test); (F) Simpson index (P = 0.46, Mann-Whitney U test). We
380 obtained reprint permission from previous publishers. This figure has been modified from
381 Wang et al.[11].
382
383 **Figure 3: Relative abundance of phyla (> 1%) and of the top 12 species in ovarian samples.**
384 (A) The relative abundance of the phyla (> 1%) in the ovaries of the patients in the control
385 group. (B) The relative abundance of the phyla (> 1%) in the ovaries of patients with ovarian
386 cancer. (C) The relative abundances of the 12 most abundant bacterial species in the ovaries
387 of the control patients. (D) The relative abundances of the 12 most abundant bacterial species
388 in the ovaries of ovarian cancer patients. We obtained reprint permission from previous
389 publishers. This figure has been modified from Wang et al.[11].
390
391 **Figure 4: PCoA detects clusters of communities and the relative abundances of**
392 **Anoxynatronum sibiricum and Methanosarcina vacuolata.** (A) Communities were clustered
393 using PCoA. PC1 and PC2 are plotted on the x and y axes. The red block indicates a sample in
394 the ovarian cancer group. The blue circle indicates a sample in the control group. The samples
395 from the ovarian cancer group were separated from other samples in the control group. (B)
396 Communities clustered using PCoA. PC1 and PC2 are plotted on the x and y axes. The red block

397 indicates a sample in the ovarian cancer group. The blue solid circle indicates a sample from a
398 patient with uterine myoma, and the blue hollow circle is equal to a sample of a patient with
399 uterine adenomyosis. (C) The relative abundance of *Anoxynatronum sibiricum* (control group:
400 n = 10, cancer group: n = 6, P = 0.034, Mann-Whitney U test). (D) The relative abundance of
401 *Methanosarcina vacuolata* (control group: n = 10, cancer group: n = 6, P = 0.001, Mann-
402 Whitney U test). We obtained reprint permission from previous publishers. This figure has
403 been modified from Wang et al.[11].
404
405 **Figure 5: Predicted metagenomes analyzed by BugBase.** The expression of some genes in the
406 cancer group was increased compared with that in the control group. These genes were
407 related to potentially pathogenic (Wilcoxon signed-rank test, P = 0.02) and oxidative stress-
408 tolerant phenotypes of the ovaries. (Wilcoxon signed-rank test, P = 0.002). We obtained
409 reprint permission from previous publishers. This figure has been modified from Wang et al.[11].
410
411 **Figure 6: PICRUSt analysis of different KEGG pathways between the cancer and control**
412 **groups.** We obtained reprint permission from previous publishers. This figure has been
413 modified from Wang et al.[11].
414
415 Table 1: Patient statistics
416
417 Table 2: Richness (represented by the Chao 1 and ACE index) and the diversity (represented by
418 the Shannon, Simpson, and Evenness index) of the bacterial species
419
420 **DISCUSSION:**
421 Ovarian cancer has a notable influence on women's fertility[25]. Most ovarian cancer patients
422 are diagnosed at late stages, and the 5-year survival rate is less than 30%[18]. Confirmation of
423 bacteria in the abdominal solid viscera, including the liver, pancreas and spleen, has been
424 published. The existence of bacteria in the upper female reproductive tract occurs because the
425 cervix is not enclosed[2-5]. However, whether ovaries, which are abdominal solid viscera, are
426 sterile or not has not yet been determined. Additionally, whether bacteria in the ovaries are
427 related to ovarian cancer is also an important question.
428
429 The significant differences in the bacteria that we found were compared between different
430 groups. All of the procedures mentioned above were strictly germfree, including instruments,
431 reagents, equipment, and the operation of the whole protocol. More importantly, we used
432 ovaries from patients with benign uterine disease as the control group to counteract possible
433 contamination. However, in this protocol, contamination cannot be avoided. Thus, since the
434 cancer group and control group were analyzed in the same experimental environment, merely
435 by comparing the differences between these two groups, we could obtain primary evidence
436 about the microbiological origin of ovarian cancer.
437
438 The findings of bacteria in ovarian tissue might start a new field investigating the bacteria
439 influencing ovarian cancer. Additionally, the unique presence and composition of bacteria in
440 cancerous ovarian tissues might direct the carcinogenesis of ovarian cancer, and the

therapeutic and prognostic targets of bacteria. Among the 46 KEGG pathways, functions related to the biosynthesis of vancomycin group antibiotics drew particular attention. This may provide further treatment options for ovarian cancer.

However, the protocol had some limitations. First, the samples could not be collected from healthy people for ethical reasons. The control group was ovaries of patients with benign uterine disease (including uterine myoma and adenomyosis). Second, the number of samples should be larger. The limited sample size of the study might hamper the accuracy of the results. Third, although the cancer group and the control group were under the same conditions, there were no negative or positive controls. In addition, contamination could not be avoided. To date, the study of the ovarian bacteria in patients with ovarian cancer is still in an early stage. A larger-scale study with more samples is needed.

ACKNOWLEDGMENTS:
This work was supported by the Clinical Research Award of the First Affiliated Hospital of Xi'an Jiaotong University, China (XJTU1AF-2018-017, XJTU1AF-CRF-2019-002), the Major Basic Research Project of Natural Science of Shaanxi Provincial Science and Technology Department (2018JM7073, 2017ZDJC-11), the Key Research and Development Project of Shaanxi Provincial Science and Technology Department (2017ZDXM-SF-068, 2019QYPY-138), the Shaanxi Provincial Collaborative Technology Innovation Project (2017XT-026, 2018XT-002), and the Medical Research Project of Xi'an Social Development Guidance Plan (2017117SF/YX011-3). The funders had no role in study design, data collection and analysis, decision to publish, or preparation of the manuscript.

We thank the colleagues in the Department of Gynecology of First Affiliated Hospital of Xi'an Jiaotong University for their contributions to collecting samples.

DISCLOSURES:
The authors have nothing to disclose.

REFERENCES:
1 Manfredo Vieira, S. *et al.* Translocation of a gut pathobiont drives autoimmunity in mice and humans. *Science.* **359** (6380), 1156-1161 (2018).
2 Geller, L. T. *et al.* Potential role of intratumor bacteria in mediating tumor resistance to the chemotherapeutic drug gemcitabine. *Science.* **357** (6356), 1156-1160 (2017).
3 Manfredo, V. S. *et al.* Translocation of a gut pathobiont drives autoimmunity in mice and humans. *Science.* **359** (6380), 1156-1161 (2018).
4 Brunelli, R. *et al.* Globular structure of human ovulatory cervical mucus. *FASEB J.* **21** (14), 3872-3876 (2007).
5 Chen, C. *et al.* The microbiota continuum along the female reproductive tract and its relation to uterine-related diseases. *Nature Communications.* **8** (1), 875 (2017).
6 Zervomanolakis, I. *et al.* Physiology of upward transport in the human female genital tract. *Annals of the New York Academy of Sciences.* **1101**, 1-20 (2007).
7 Verstraelen, H. *et al.* Characterisation of the human uterine microbiome in non-

pregnant women through deep sequencing of the V1-2 region of the 16S rRNA gene. *PeerJ.* **4**, e1602 (2016).

8 Fang, R. L. *et al.* Barcoded sequencing reveals diverse intrauterine microbiomes in patients suffering with endometrial polyps. *American Journal of Translational Research.* **8** (3), 1581-1592 (2016).

9 Miles, S. M., Hardy, B. L. & Merrell, D. S. Investigation of the microbiota of the reproductive tract in women undergoing a total hysterectomy and bilateral salpingo-oopherectomy. *Fertil Steril.* **107** (3), 813-820 e811 (2017).

10 Banerjee, S. *et al.* The ovarian cancer oncobiome. *Oncotarget.* **8** (22), 36225-36245 (2017).

11 Wang, Q. *et al.* The differential distribution of bacteria between cancerous and noncancerous ovarian tissues in situ. *Journal of Ovarian Research.* **13** (1), 8 (2020).

12 Wang, L. *et al.* Bacterial overgrowth and diversification of microbiota in gastric cancer. *European Journal of Gastroenterology & Hepatology.* **28** (3), 261-266 (2016).

13 Hosgood, H. D., 3rd *et al.* The potential role of lung microbiota in lung cancer attributed to household coal burning exposures. *Environmental and Molecular Mutagenesis.* **55** (8), 643-651 (2014).

14 Kwon, M., Seo, S. S., Kim, M. K., Lee, D. O. & Lim, M. C. Compositional and Functional Differences between Microbiota and Cervical Carcinogenesis as Identified by Shotgun Metagenomic Sequencing. *Cancers*. **11** (3), 309 (2019).

15 Urbaniak, C. *et al.* The Microbiota of Breast Tissue and Its Association with Breast Cancer. *Applied and Environmental Microbiology.* **82** (16), 5039-5048 (2016).

16 Feng, Y. *et al.* Metagenomic and metatranscriptomic analysis of human prostate microbiota from patients with prostate cancer. *BMC Genomics.* **20** (1), 146 (2019).

17 Walsh, D. M. *et al.* Postmenopause as a key factor in the composition of the Endometrial Cancer Microbiome (ECbiome). *Scientific Reports.* **9** (1), 19213 (2019).

18 Walther-Antonio, M. R. *et al.* Potential contribution of the uterine microbiome in the development of endometrial cancer. *Genome Medicine.* **8** (1), 122 (2016).

19 Poore, G. D. *et al.* Microbiome analyses of blood and tissues suggest cancer diagnostic approach. *Nature.* **579** (7800), 567-574 (2020).

20 Bolger, A. M., Lohse, M. & Usadel, B. Trimmomatic: a flexible trimmer for Illumina sequence data. *Bioinformatics.* **30** (15), 2114-2120 (2014).

21 Ward, T. *et al.* BugBase predicts organism-level microbiome phenotypes. *bioRxiv.* 10.1101/133462 133462 (2017).

22 Langille, M. G. *et al.* Predictive functional profiling of microbial communities using 16S rRNA marker gene sequences. *Nature Biotechnology.* **31** (9), 814-821 (2013).

23 Langille, M. G. I. *et al.* Predictive functional profiling of microbial communities using 16S rRNA marker gene sequences. *Nature Biotechnology.* **31** (9), 814 (2013).

24 Parks, D. H., Tyson, G. W., Hugenholtz, P. & Beiko, R. G. STAMP: statistical analysis of taxonomic and functional profiles. *Bioinformatics.* **30** (21), 3123 (2014).

25 Leranth, C. & Hamori, J. "Dark" Purkinje cells of the cerebellar cortex. *Acta Biologica Hungarica.* **21** (4), 405-419 (1970).

Figure 1

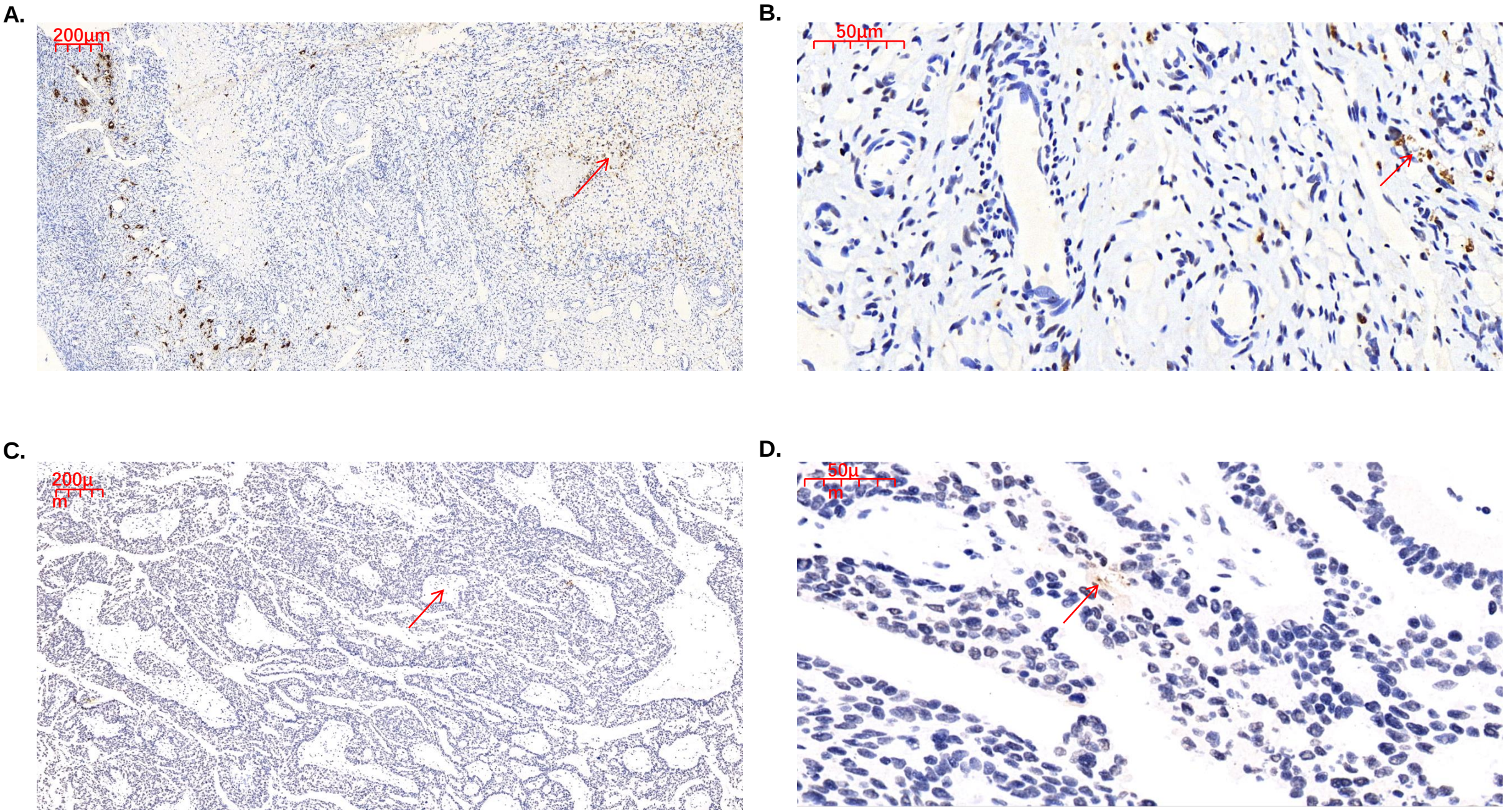

Figure 2

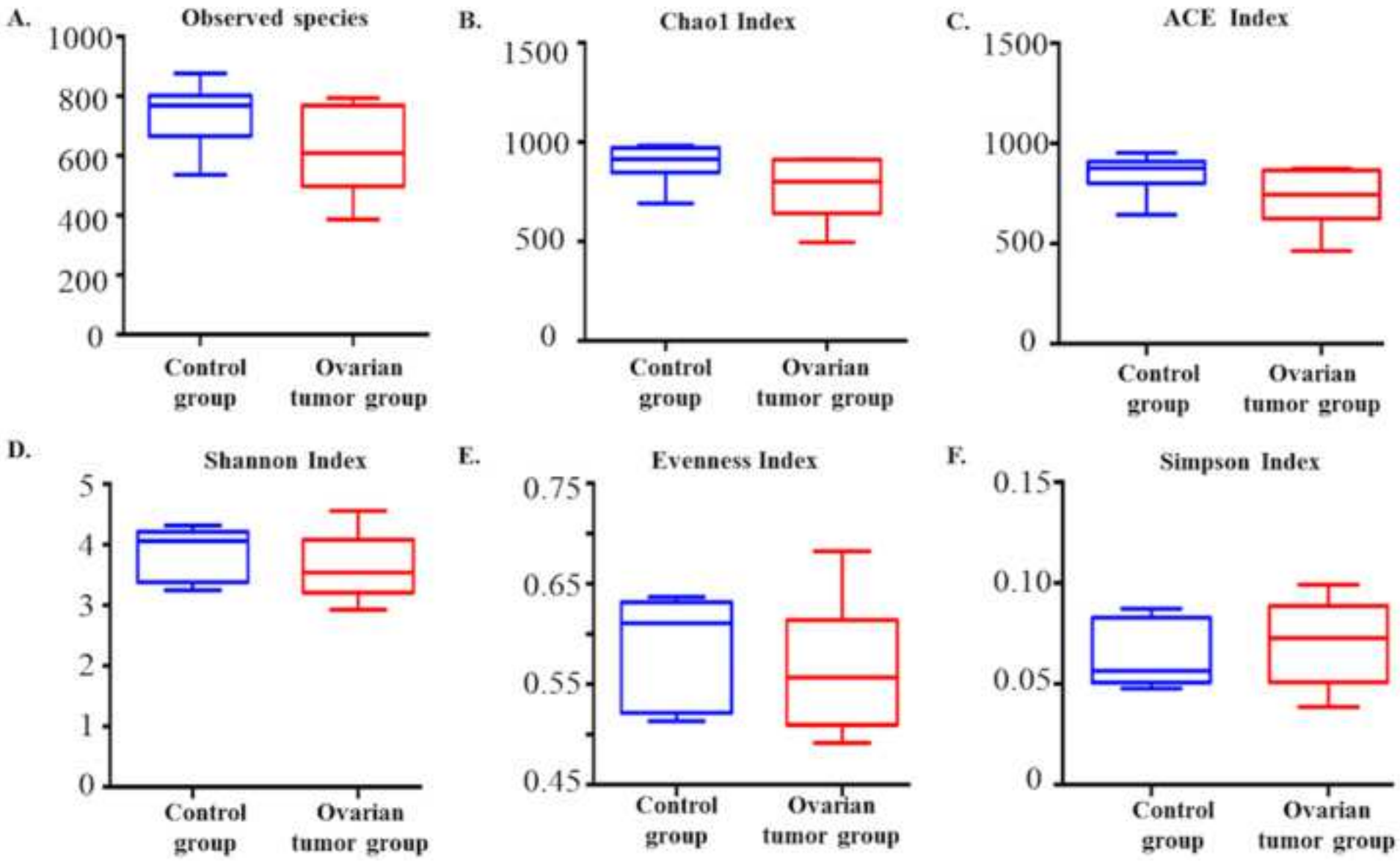

Figure 3

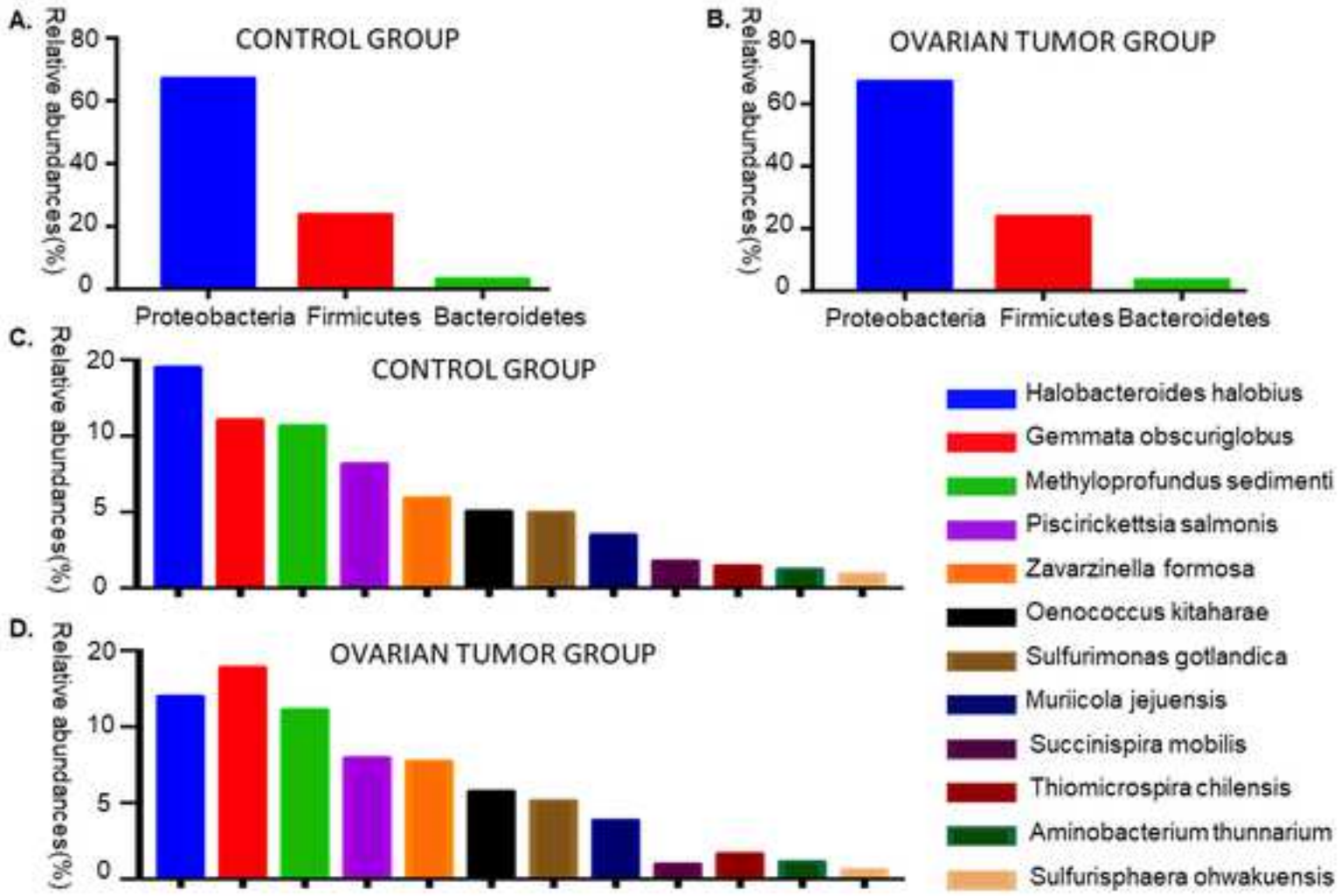

Figure 4

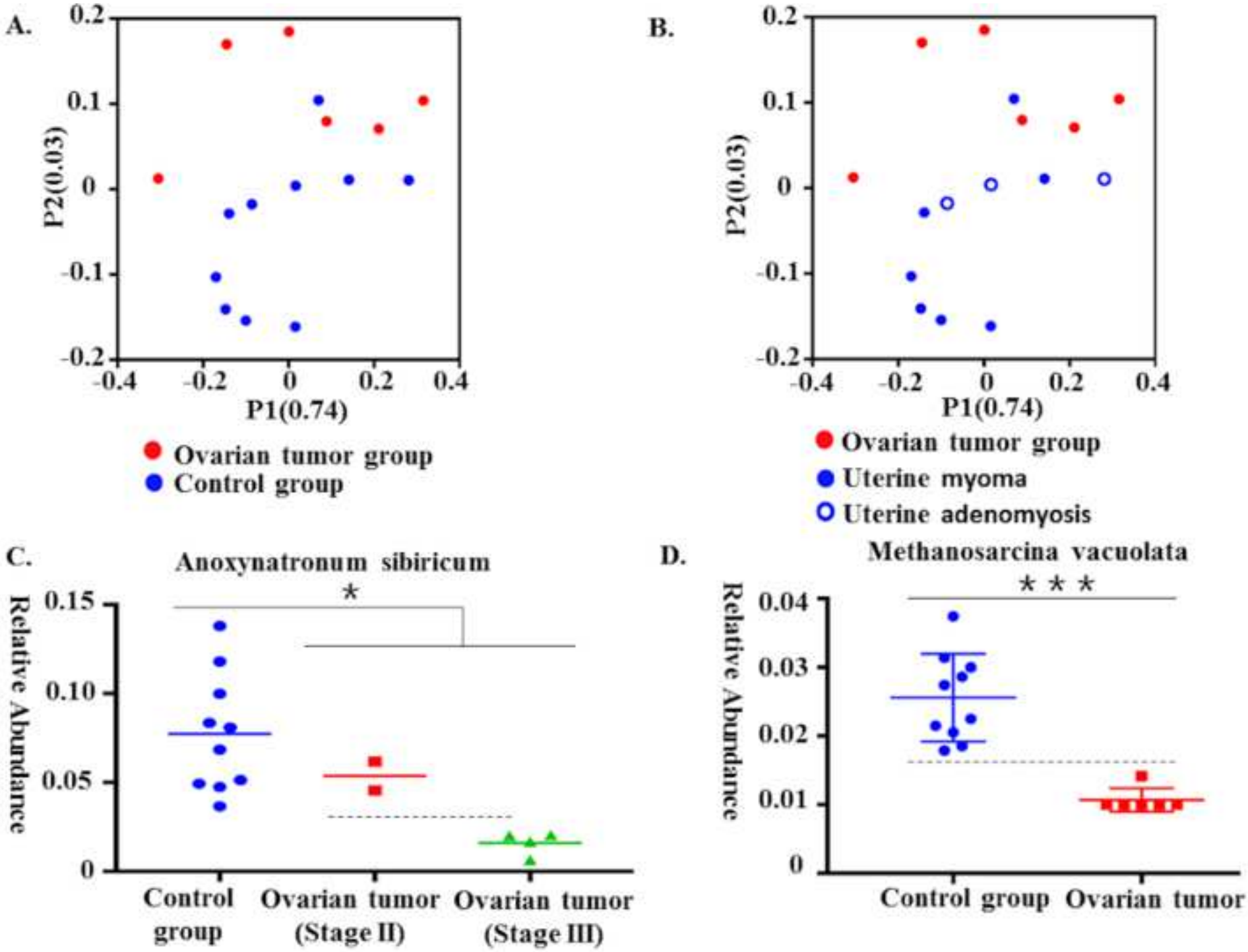

Figure 5

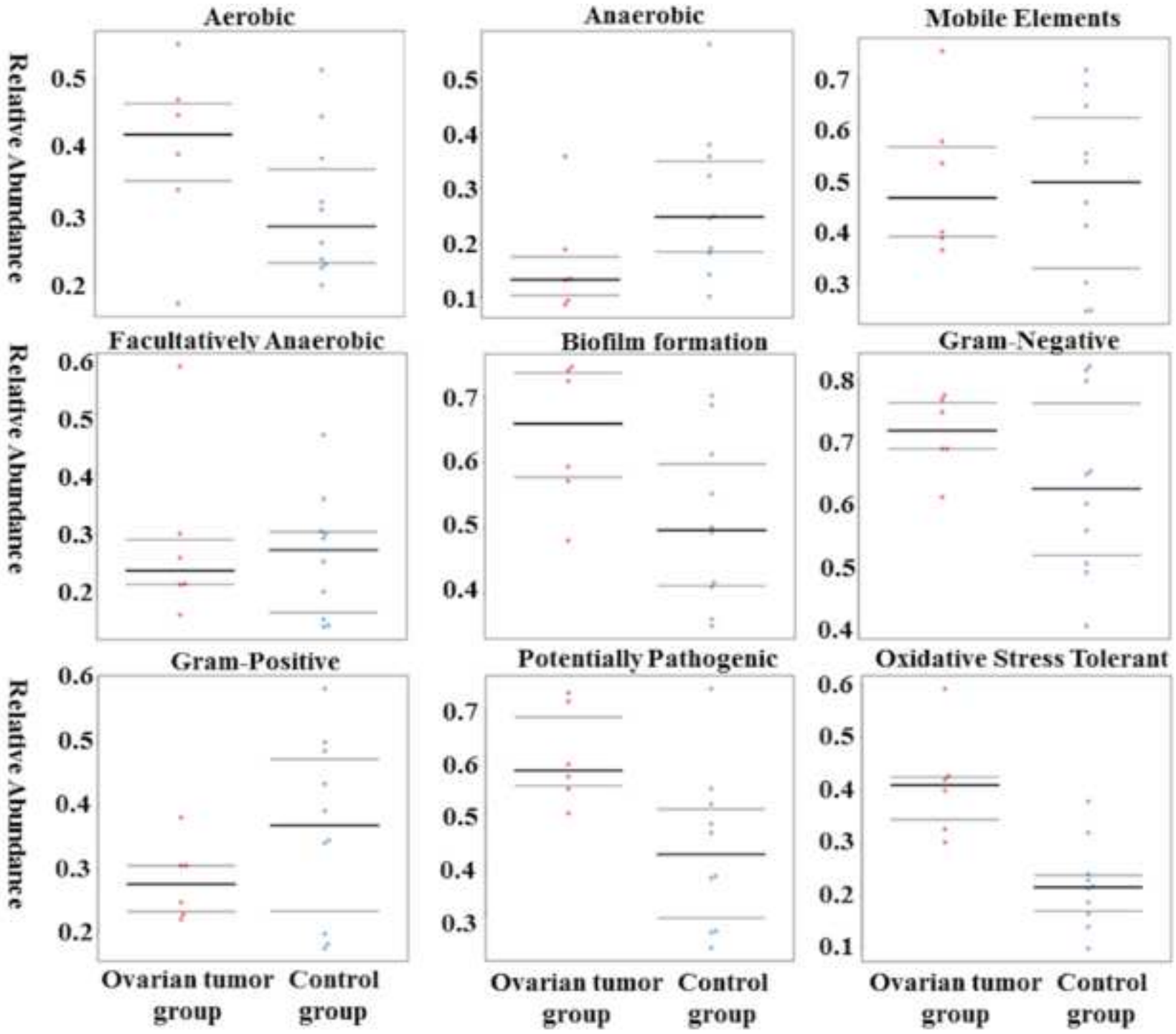

Figure 6

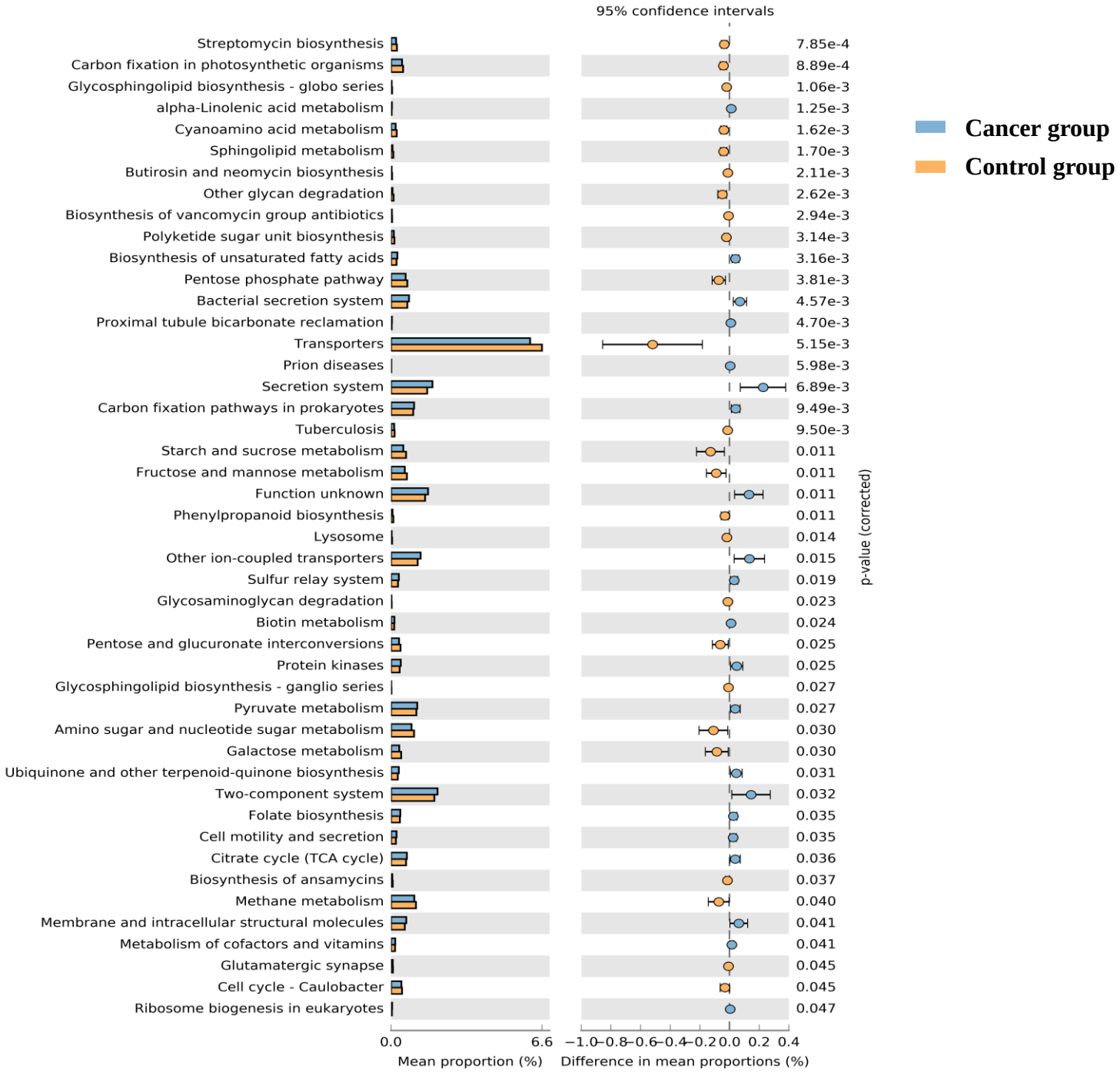

Table 1

	Control group (n=10)	Cancer group (n=6)	P value
Age	51.6 (45-57)	57.3 (46-75)	0.29
Menopausal status			0.12
Pre/Peri	8	2	
Post	2	4	
Parity	5.1 (1-13)	3.1 (2-5)	0.17
History of hypertension			0.52
Yes	1	2	
No	9	4	
History of diabetes			0.7
Yes	1	1	
No	9	5	
Stage (%)			
Ⅱ		2 (33.3)	
Ⅲ		4 (66.7)	
Histotype (%)			
Uterine myoma	3 (30)	-	
Uterine adenomyosis	7 (70)	-	
Ovarian serous carcinoma	-	6 (100)	

Table 2

		Control cohort (n=10, %)	Ovarian tumor cohort (n = 6, %)	P value
Phylum	Planctomycetes	0.5144 ± 0.1420	0.8655 ± 0.2638	0.023
	Crenarchaeota	0.2840 ± 0.0787	0.1592 ± 0.0775	0.023
	Aquificae	0.0352 ± 0.0137	0.0697 ± 0.0291	0.017
Class	Spartobacteria	0.3149 ± 0.0923	0.4795 ± 0.1205	0.026
	Sphingobacteriia	0.1280 ± 0.0695	0.0423 ± 0.0706	0.039
Order	Planctomycetales	7.2700 ± 1.3880	9.1183 ± 0.8594	0.039
	Pseudomonadales	0.1332 ± 0.0746	0.4283 ± 0.4019	0.023
	Enterobacteriales	0.6038 ± 0.1237	2.0105 ± 2.5829	0.03
	Methanobacteriales	0.1626 ± 0.0496	0.2602 ± 0.0859	0.03
	Halobacteriales	0.0648 ± 0.0117	0.0439 ± 0.0287	0.039
	Campylobacterales	0.0776 ± 0.0158	0.1133 ± 0.0232	0.009
Family	Flavobacteriaceae	24.7500 ± 0.6712	21.7167 ± 3.0732	0.014
	Methanobacteriaceae	0.1720 ± 0.0540	0.2667 ± 0.0867	0.039
	Moraxellaceae	0.1328 ± 0.0658	0.4347 ± 0.4054	0.03
	Petrotogaceae	0.0452 ± 0.0178	0.0638 ± 0.0112	0.039
	Thermaceae	0.0078 ± 0.0089	0.0188 ± 0.0086	0.017

	Archaeoglobaceae	0.0611 ± 0.0221	0.0381 ± 0.0123	0.045
	Leptotrichiaceae	0.1018 ± 0.0524	0.0442 ± 0.0284	0.03
	Microbacteriaceae	0.1493 ± 0.0618	0.2740 ± 0.1320	0.039
	Staphylococcaceae	0.0281 ± 0.0545	0.0822 ± 0.0536	0.029
	Thermogemmatisporaceae	0.7381 ± 0.1925	1.4583 ± 0.6982	0.013
	Methanocorpusculaceae	0.0233 ± 0.0139	0.0091 ± 0.0063	0.023
	Geodermatophilaceae	0.0552 ± 0.0335	0.0144 ± 0.0145	0.03
Genus	Paenibacillus	0.7990 ± 0.4563	0.3207 ± 0.2151	0.039
	Haloferula	0.1811 ± 0.0623	0.1156 ± 0.0263	0.023
	Subdivision	0.0801 ± 0.0314	0.0465 ± 0.0188	0.039
	Zavarzinella	0.0741 ± 0.0238	0.1234 ± 0.0305	0.009
	Photorhabdus	0.0013 ± 0.0029	0.0068 ± 0.0050	0.023
	Volucribacter	0.0081 ± 0.0062	0.0021 ± 0.0046	0.042
	Blastococcus	0.0552 ± 0.0335	0.0144 ± 0.0145	0.03
	Mesotoga	0.2509 ± 0.0703	0.3675 ± 0.1057	0.039
	Defluviitoga	0.0550 ± 0.0252	0.0216 ± 0.0114	0.03
	Dorea	0.0063 ± 0.0065	0.0000 ± 0.0000	0.025
Species	Rhodopirellularubra	0.4011 ± 0.1433	0.7563 ± 0.2398	0.013

Haloferulasargassicola	0.1534 ± 0.0629	0.0999 ± 0.0227	0.03
Thermogematisporafoliorum	0.7813 ± 0.2152	1.4957 ± 0.6735	0.023
Mycoplasmaequigenitalium	0.5463 ± 0.0684	0.6820 ± 0.1108	0.039
Bifidobacteriumsubtile	0.0924 ± 0.0269	0.2584 ± 0.1958	0.026
Natronielaacetigena	0.0075 ± 0.0078	0.0000 ± 0.0000	0.012
Flammeovirgakamogawensis	0.6966 ± 0.3523	0.2488 ± 0.1349	0.026
Eubacteriumyurii	0.0231 ± 0.0111	0.0091 ± 0.0074	0.03
Enterococcusdiestrammenae	0.2549 ± 0.0859	0.1458 ± 0.0809	0.03
Pelagicoccusalbus	0.0127 ± 0.0057	0.0047 ± 0.0024	0.017
Fodinibacterluteus	0.1588 ± 0.0461	0.0935 ± 0.0498	0.039
Prosthecobacteralgae	0.0210 ± 0.0121	0.0080 ± 0.0050	0.03
Emticiciaoligotrophica	0.0743 ± 0.0297	0.0308 ± 0.0251	0.013
Leuconostoccitreum	0.0417 ± 0.0281	0.0108 ± 0.0125	0.039
Methanimicrococcusblatticola	0.2138 ± 0.0527	0.1572 ± 0.0383	0.039
Methanosarcinavacuolata	0.0156 ± 0.0061	0.0007 ± 0.0015	0.001
Lactobacillussucicola	0.0160 ± 0.0063	0.0081 ± 0.0053	0.03
Caldicoprobacterosshimai	0.0014 ± 0.0041	0.0044 ± 0.0042	0.048

Caldicellulosiruptor saccharolyticus	0.3268 ± 0.1880	0.1082 ± 0.1296	0.039
Methylomicrobium album	0.0013 ± 0.0021	0.0069 ± 0.0051	0.013
Novispirillum itersonii	0.0031 ± 0.0036	0.0000 ± 0.0000	0.048
Paenibacillus odorifer	0.6905 ± 0.4128	0.2356 ± 0.1583	0.039
Mycoplasma genitalium	0.0023 ± 0.0038	0.0073 ± 0.0048	0.043
Sulfurospirillum halorespirans	0.0630 ± 0.0163	0.0948 ± 0.0306	0.039
Streptococcus caseoreus	0.0514 ± 0.0415	0.0190 ± 0.0329	0.03
Spongiivirga citrea	0.2355 ± 0.1391	0.0921 ± 0.0784	0.039
Staphylococcus capitis subsp	0.0245 ± 0.0504	0.0752 ± 0.0506	0.021
Xanthomonas bromi	0.0094 ± 0.0117	0.0000 ± 0.0000	0.025
Vulcanisaeta thermophila	0.0457 ± 0.0106	0.0720 ± 0.0247	0.039
Volucribacter amazonae	0.0081 ± 0.0062	0.0021 ± 0.0046	0.042
Thalassotalea fusca	0.0316 ± 0.0202	0.0027 ± 0.0045	0.004
Thermus islandicus	0.0051 ± 0.0049	0.0000 ± 0.0000	0.025
Prevotella veroralis	0.0055 ± 0.0074	0.0000 ± 0.0000	0.048

Pseudobutyrivibrio xylanivorans	0.0072 ± 0.0063	0.0021 ± 0.0046	0.03
Peptoniphilus methioninivorax	0.0000 ± 0.0000	0.0031 ± 0.0033	0.017
Sphingobacterium arenae	0.2488 ± 0.1235	0.0861 ± 0.0529	0.03
Campylobacter rectus	0.0050 ± 0.0064	0.0000 ± 0.0000	0.048
Blautia glucerasea	0.0166 ± 0.0091	0.0056 ± 0.0067	0.033
Calditerricola yamamurae	0.0745 ± 0.0158	0.1084 ± 0.0306	0.023
Clostridium thermosuccinogenes	0.0036 ± 0.0051	0.0127 ± 0.0089	0.03
Alkalibacillus haloalkaliphilus	0.0058 ± 0.0066	0.0000 ± 0.0000	0.025
Acholeplasma oculi	0.0038 ± 0.0041	0.0000 ± 0.0000	0.025
Aureimonas phyllosphaerae	0.0013 ± 0.0029	0.0068 ± 0.0050	0.023
Azonexus hydrophilus	0.0773 ± 0.0316	0.0285 ± 0.0190	0.007
Anaerostipes rhamnosivorans	0.0005 ± 0.0015	0.0045 ± 0.0043	0.025
Anoxynatronum sibiricum	0.1172 ± 0.0708	0.0460 ± 0.0513	0.034
Legionella taurinensis	0.0029 ± 0.0031	0.0000 ± 0.0000	0.048

Mesonia phycicola	0.0119 ± 0.0087	0.0031 ± 0.0033	0.019
Luteolibacter cuticulihirudinis	0.2389 ± 0.1090	0.4292 ± 0.1517	0.03
Megasphaera indica	0.0052 ± 0.0055	0.0000 ± 0.0000	0.025
Dorea formicigenerans	0.0063 ± 0.0065	0.0000 ± 0.0000	0.025
Fuchsiella alkaliacetigena	0.0082 ± 0.0075	0.0014 ± 0.0031	0.043
Geobacillus thermodenitrificans	0.0063 ± 0.0051	0.0006 ± 0.0013	0.024

Click here to access/download

Table of Materials

JoVE_Table_of_Materials.xlsx

Editorial comments:

Changes to be made by the Author(s) regarding the written manuscript:
None.

Changes to be made by the Author(s) regarding the video:
Composition
08:41 - A random black border appears during this figure. Please make the background all white so we don't see the edge of the figure.

Please upload a revised high-resolution video here:
https://www.dropbox.com/request/DYGKknA7Z8tk598ICK1w?oref=e
or
https://www.jove.com/account/file-uploader?src=18872838
or
any way you can and I can download the revised video.
Response: Thank you for your suggestion. We have submitted our latest video.

June 26, 2021

Dear Zhao,

Thank you for your letter. I have known that your under-reviewed protocol "Characterization of Bacteria in Ovarian Tissues and Functional Prediction of These Bacteria" has some figures reprinted from the article "The differential distribution of bacteria between cancerous and noncancerous ovarian tissues in situ". We permitted the reprint.

Sincerely,

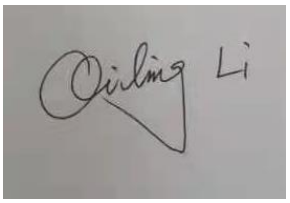

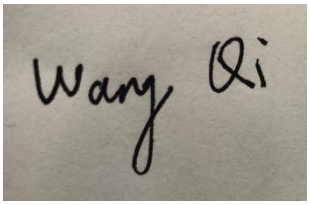

Qiling Li

ELSEVIER

Certificate of Elsevier Language Editing Services

The following article was edited by Elsevier Language Editing Services:

"Characterization of Bacteria in Ovarian Tissues and Functional Prediction of These Bacteria"

Authored by:

Qiling Li

Date: 19-Jul-2021
Serial number: LE-216501-9A68E386AADE